JOURNAL OF SOLID STATE CHEMISTRY 115, 499–507 (1995)

Structure and Oxygen Stoichiometry in $Sr_3Co_2O_{7-y}$ ($0.94 \leq y \leq 1.22$)

S. E. Dann and M. T. Weller[1]

Department of Chemistry, University of Southampton, Highfield, Southampton SO9 5NH, United Kingdom

Received May 12, 1994, in revised form July 5, 1994; accepted July 11, 1994

A new, oxygen-deficient Ruddlesden–Popper phase, $Sr_3Co_2O_{7-y}$ ($0.94 \leq y \leq 1.22$) has been prepared and its structural characterization has been achieved by the Rietveld refinement of powder X-ray and powder neutron diffraction data. At low y the system is tetragonal but as y increases a phase change to orthorhombic occurs. $Sr_3Co_2O_{6.06}$ crystallizes in the space group *I4/mmm*, adopting the $Sr_3Ti_2O_7$ type structure, but with the oxygen vacancies lying exclusively on the site linking the CoO_6 octahedra. This leads to an unusual square-pyramidal coordination for Co(III). The orthorhombic structures of the samples $y = 1.22$ and $y = 1.06$ have been determined using powder neutron diffraction. Crystallizing in the space group *Immm*, the ordering of oxygen vacancies in the Ruddlesden–Popper phase, leads to a threefold tripling along the *b*-axis direction.

INTRODUCTION

Strongly oxidizing conditions are required to produce stoichiometric cobalt(IV) materials. $SrCoO_3$ was first synthesized as a stoichiometric cubic phase in 1985 by reaction of CoO and $SrCO_3$ using an anvil device and a pressure of 65 Kbar with $KClO_3$ as the oxygen source (1). This can be contrasted to $SrFeO_3$ (2), which requires a much lower pressure for synthesis, ca. 800 bar. Few other cobalt(IV) compounds are reported in the literature but mixed valence compounds containing both cobalt(III) and cobalt(IV) are more common. These can be generated formally from cobalt(IV) compounds, e.g., $SrCoO_3$, either by doping in trivalent cations, e.g., $La_{1-x}Sr_xCoO_3$ (3), or by using low pressure routes to introduce oxygen vacancies, e.g., $SrCoO_{2.7}$ (4).

While cobalt(IV) compounds are rare, more complex structures containing a tetravalent transition, metal ion, strontium, and oxygen (5, 6) have been shown to form for iron: for example, those crystallizing with the K_2NiF_4 (Sr_2FeO_4) (7) and the $Sr_3Ti_2O_7$ ($Sr_3Fe_2O_7$) (8) structures. The oxidation state of the transition metal cation in these structures can be reduced to below four; for example, in the Ruddlesden–Popper phase $Sr_3Fe_2O_7$ (Fig. 1) systematic removal of oxygen from the O3 (0, 0, 0) site produces a novel square-pyramidal coordination of the trivalent ion when the stoichiometry reaches 6, although the tetragonal crystal system is retained. High levels of oxygen deficiency are tolerated in other $A_3B_2O_{7-q}$ systems. For example, Nguyen *et al.* (9) showed by powder X-ray diffraction studies that the compounds, $La_{2-x}Sr_{1+x}Cu_2O_{6+y}$ (*Ln*212), have a structure derived from $Sr_3Ti_2O_7$. When $y = 0$, the copper atoms in the system have a square-pyramidal coordination with four short basal Cu–O bonds and one long apical Cu–O distance with the O3 site vacant. Further oxygen deficiencies in the perovskite layers, ($y \leq 0$), result in two-dimensional CuO_2 planes with removal of oxygen from the O2 (0, 0, z) site.

Nguyen extended this work by considering $Ln_{2-x}Sr_{1+x}Cu_2O_{6-y}$ (*Ln*636), where *Ln* = Sm, Gd, $0.7 \leq x \leq 0.9$ and Eu, $0.6 \leq x \leq 0.9$ (10), which resulted in semiconducting materials with a threefold superstructure along the *b*-axis, caused by both cation and oxygen ordering. The other notable attribute was that the oxygen stoichiometry was now much reduced below 6 i.e., $0.45 \leq y \leq 0.3$. A structural model (Fig. 2) was proposed from X-ray data although considering the complexity of the structure and the limited amount of data available, a high level of uncertainty in the oxygen positions and occupancy factors resulted. A neutron diffraction study of these systems was not performed by Nguyen due to the high level of absorbtion of neutrons by all of these lanthanide nuclei. Grasmeder and Weller (11) prepared and then studied compounds in the system $Nd_{1.4}Sr_{1.6}Cu_2O_{6\pm y}$ by powder X-ray and neutron diffraction. The structural model, proposed by Nguyen for the tripled structure, was confirmed for this compound although the ordering of cations and anionic vacancies was quite different with the lanthanide exclusively favoring the low coordination sites. An oxygen vacancy had previously been suggested by the X-ray diffraction study and was thought to give alternating $A_1Cu(2)O_3$ and $A_2Cu(1)O_2$ blocks. However, neutron refinement in the $Nd_{1.4}Sr_{1.6}Cu_2O_{6\pm y}$ system showed the ordering to be more complex: oxygen vacancies produced discontinuities in the CuO_2 planes in the *b*-direction. Vertex-linked CuO_5 square pyramids, which form six-mem-

[1] To whom correspondence should be addressed.

0022-4596/95 $6.00

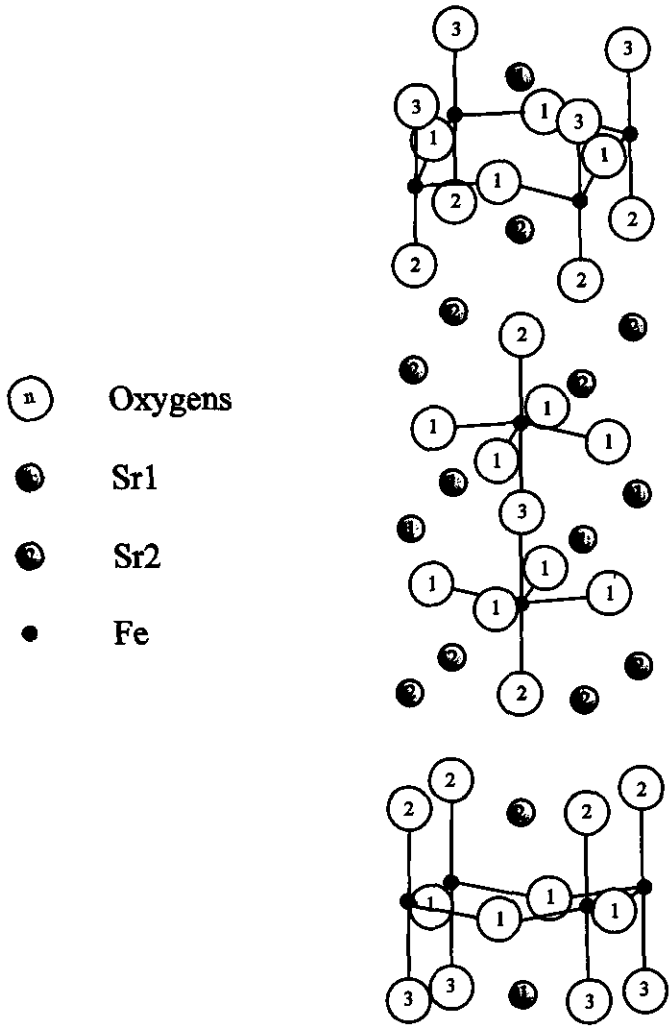

FIG. 1. The structure of $Sr_3Fe_2O_7$ showing the two strontium sites and octahedral coordination to iron.

bered rings by corner sharing, constructed rectangular tunnels running parallel to the *a*-direction. These tunnels were partially empty due to oxygen absences on the O7 site. Occupation of the O7 site results in a Cu1–O7–Cu1 link which bridges the tunnel with a very short Cu1–O7 contact distance.

This paper reports the preparation of a new phase $Sr_3Co_2O_{7-y}$, generated using high temperature and ambient pressure. This previously unknown phase, $Sr_3Co_2O_{7-y}$ ($0.94 \leq y \leq 1.22$), was identified by comparison with other materials with structures based on the $Sr_3Ti_2O_7$ structure (8) and characterized using powder diffraction methods. Accurate structure determination was carried out using powder neutron diffraction on the high resolution powder diffractometer (HRPD) at the Rutherford Appleton Laboratory. The oxygen content was determined by thermogravimetric analysis and the refinement of oxygen occupancies from powder neutron diffraction data.

EXPERIMENTAL

A sample of $Sr_3Co_2O_{7-z}$ was synthesized by direct solid state reaction of $SrCO_3$ (99.9%) and CoO (99.99%), in a molar ratio of 3 : 2 heated at 1000°C in a box furnace for 24 hr. After air quenching and regrinding, samples of this compound were then treated further to control the oxygen stoichiometry, as shown in Table 1.

Powder X-ray diffraction data were collected on the products of the annealing experiments; the data showed

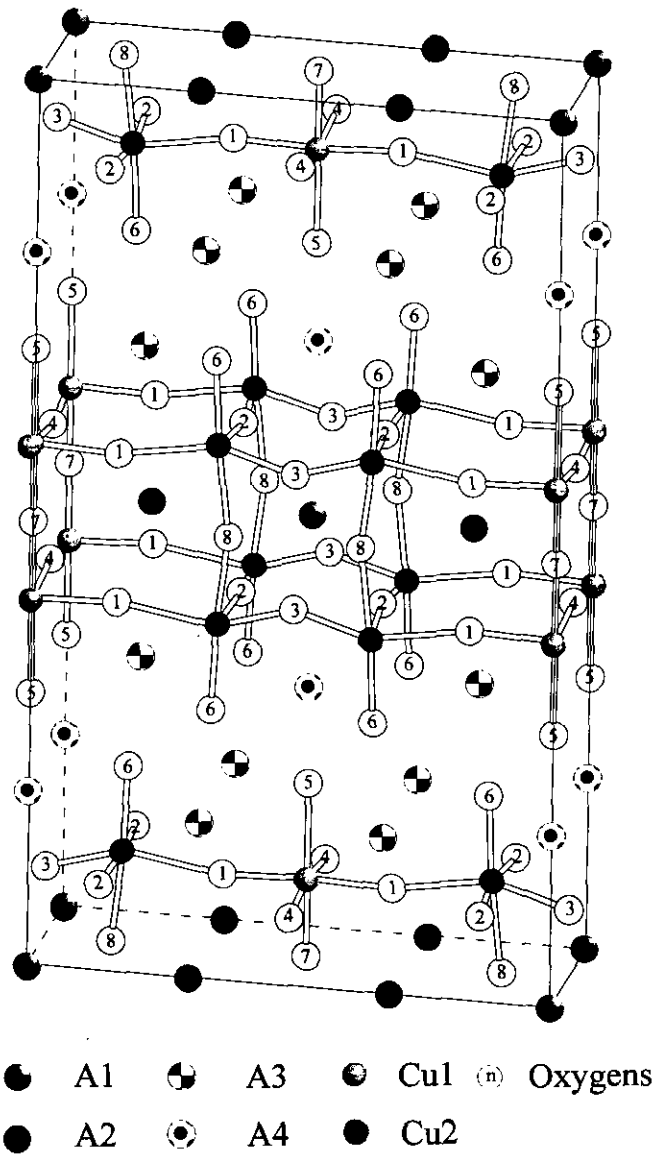

FIG. 2. The structure of the $Ln_{2-x}Sr_{1+x}Cu_2O_{6-y}$ (Ln = Sm, $0.7 \leq x \leq 0.9$) formed by tripling of the Ruddlesden–Popper phase in the *b*-direction.

TABLE 1
Annealing Treatment

Treatment	a/b (Å)	c (Å)	3 a/b	$7 - y$
Air/1200°C Quenched	a = 3.864(1) b = 11.435(4)	20.233(9)	1.014	5.78(5)
O_2/1000°C Slow cool/440°C Quenched	a = 3.838(1) b = 11.492(3)	20.099(10)	1.002	5.94(5)
O_2/1000°C Slow cool/200°	a = 3.830(3) b = 3.830(3)	20.075(11)	1.000	6.06(5)

the samples to be single phase (Fig. 3). Oxygen content was determined by thermogravimetric analysis (TGA) under 5% H_2/N_2 in platinum crucibles heated to 1000°C. Powder X-ray diffraction analysis of the TGA product showed a mixture of SrO and an amorphous phase, with metallic behavior, which was assumed to be cobalt metal. The analytically determined oxygen content will be used hereafter to describe the samples. Annealing of samples at temperatures lower than 480°C caused deterioration of the sample crystallinity and sample decomposition.

Close scrutiny of the X-ray diffraction patterns of the samples, $7 - y = 5.78$, 5.94, and 6.06, revealed a change in structure as the oxygen content increased above 6 (Fig. 3). On this basis, it was decided to collected powder X-ray diffraction data over an extended period, for structure refinement on samples from the two structural regions.

Powder X-ray diffraction data were collected on the samples $7 - y = 5.78$ and 6.06 sealed in aluminum sample holders under Mylar. A step size of 0.02° in the 2θ range 30°–120° was employed to collect data over a period of 15 hr. The final profiles were of good quality although the low angle reflections, in the range 10°–30°, were obscured by the absorption of the amorphous Mylar film. In the case of the tetragonal sample, $Sr_3Co_2O_{6.06}$, there were no additional reflections in the diffraction pattern to suggest orthorhombic symmetry, but there was some evidence of line broadening in the $h00$ reflections indicative of some inhomogeneous crystallinity. Refinements were undertaken using the DBW-9006pc program running locally on personal computers using the Rietveld method (12).

In order to fully investigate the orthorhombic structure, particularly the oxygen positions, powder neutron diffraction data were collected using the high resolution diffractometer HRPD on samples $7 - y = 5.78$ and 5.94. Due to the low flux of HRPD (which receives only one in five neutron pulses from the source), large samples *ca.* 5 g were synthesized. These samples were transferred while hot to a glove box where they were separated into two specimens, one of which (0.5 g) was analyzed using powder X-ray diffraction and thermogravimetric analysis to ensure sample purity and measure the oxygen content, and the other (4–5 g) was transferred to a vanadium can and sealed with indium wire. The scattering length of cobalt is small ($b = 0.25 \times 10^{-12}$ fm^2) and consequently long collection times (>12 hr) were used to obtain the high quality data appropriate for the structure refinement

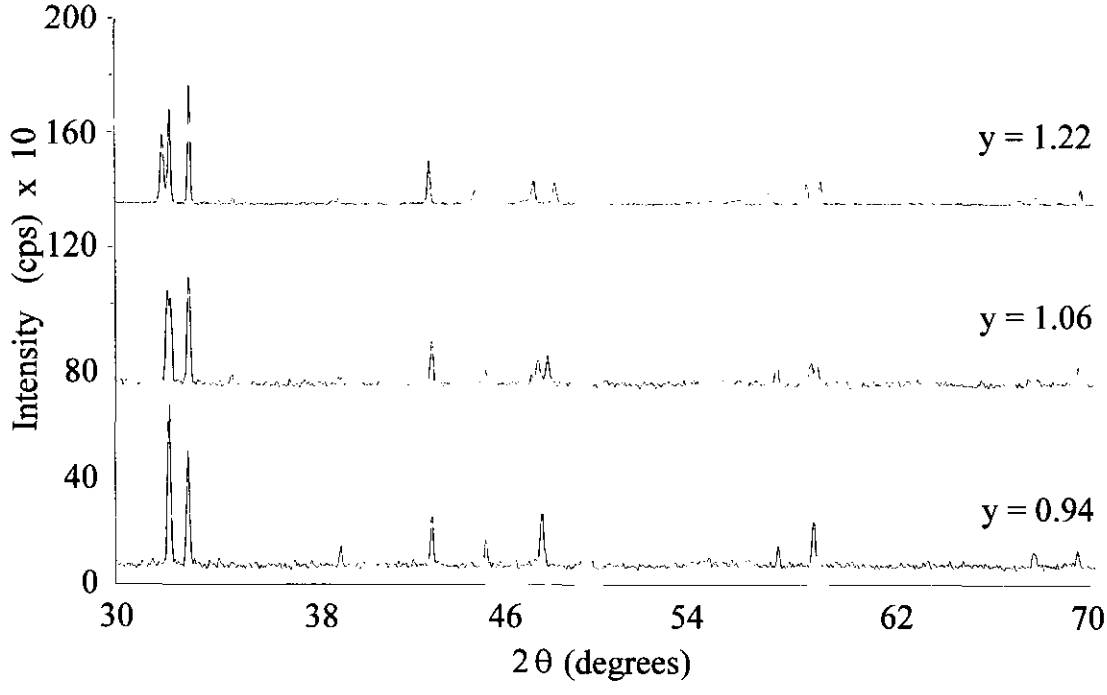

FIG. 3. X-ray patterns of the system $Sr_3Co_2O_{7-y}$ as a function of y over the 2θ range 30°–70°.

of this complex structure. A wide range, 0.6–2.2 Å, of chemically useful data were collected and the data profile was of good quality.

RESULTS AND DISCUSSION

X-Ray Structure Refinement

The structure of the air-quenched sample, $Sr_3Co_2O_{5.78}$, was refined in the space group *Immm* using the atomic coordinates of $Nd_{1.4}Sr_{1.6}Cu_2O_{5.79}$ (11) as a starting model. The tripled structure of a general $A_3B_2O_{7-q}$ phase and the labeling of sites as used in this article are given in Fig. 2. Refinement of the heavy atom positions and instrumental parameters proceeded steadily in the space group *Immm*. However, steady values could not be achieved for the oxygen positions. Evidence for low angle reflections to confirm the assignment of a tripled structure in the *b*-direction was obscured by the amorphous scattering of the Mylar film. However, indexing of all reflections was not possible without this assignment. Initially all eight oxygen sites were allowed to be fully occupied, corresponding to seven oxygens per formula unit. The oxygen occupanices refined rapidly although this was not possible without fixing isotropic temperature factors. This process suggested total vacancy on the O3 site with possible vacancies on sites O7 and O8. Refined heavy atom positions are tabulated in Table 2.

The tetragonal sample, $Sr_3Co_2O_{6.06}$, was refined in the space group *I*4/*mmm* using the parameters of $Sr_3Fe_2O_6$ (6) as a starting model. The labeling of atom sites in this structure is shown in Fig. 1. All positional parameters and isotropic temperature factors could be refined simultaneously. The occupanices of all the oxygen atoms were varied. Both the O1 and O2 sites showed only a small deviation from unity and were subsequently fixed. The O3 site refined to a partial occupancy of 0.13 producing a compound stoichiometry of $Sr_3Co_2O_{6.13}$, which was in good agreement with the analytically determined value of 6.06 (5). Essentially this suggests that most cobalt atoms in this structure are in fivefold coordination with 13% in sixfold coordination (O3 site filled). This material seems to have a similar structure to that of $Sr_3Fe_2O_6$ (6) containing square-pyramidal sheets of CoO_5 units. Refined parameters and calculated bond lengths are given in Tables 3 and 4, respectively.

TABLE 2
Heavy Atom Positions for $Sr_3Co_2O_{5.78}$ Determined by Powder X-Ray Diffraction

Atom	Site	*x*	*y*	*z*
Sr1	2*a*	0	0	0
Sr2	4*g*	0	0.3418(22)	0
Sr3	4*i*	0	0	0.1904(10)
Sr4	8*l*	0	0.3346(26)	0.1768(11)
Co1	4*i*	0	0	0.6088(15)
Co2	8*l*	0	0.3246(32)	0.6005(13)

Note. a = 3.8615(1) Å, b = 11.3894(3) Å, c = 20.2793(3) Å.

TABLE 3
Refined Atomic Parameters for $Sr_3Co_2O_{6.06}$

Atom	Site	*x*	*y*	*z*	B_{eq}	Occupancy
Sr1	2*b*	0	0	½	0.67(3)	1.00
Sr2	4*e*	0	0	0.3183(3)	0.43(6)	1.00
Co	4*e*	0	0	0.0999(6)	0.66(5)	1.00
O1	8*g*	0	¼	0.0888(4)	0.13(8)	1.00
O2	4*e*	0	0	0.1986(8)	0.75(8)	1.00
O3	2*a*	0	0	0	5.39(8)	0.13(5)

Note. a = 3.8321(1) Å, c = 20.0826(1)Å, R_{exp} = 2.86, R_{wp} = 6.04, R_p = 4.37, R_{Bragg} = 2.00.

Powder Neutron Diffraction

Examination of the patterns after data collection showed both phases, $Sr_3Co_2O_{5.78}$ and $Sr_3Co_2O_{5.94}$, to be orthorhombic and refinement proceeded in the space group *Immm*. The refined atomic positions from the X-ray refinement were used as the starting point for the neutron refinement. Refinement of the strontium and cobalt positions was achieved quickly although the latter had relatively large esd's, probably associated with the small scattering length of cobalt. Oxygen positions and isotropic temperature factors refined easily although they could not be refined simultaneously with occupancy factors. Oxygen vacancies were implied by very high temperature factors on the O3, O7, and O8 sites. The first, O3, was eventually fixed at zero, having refined the occupancy to almost zero and the temperature factors remain-

TABLE 4
Derived Bond Distances for Oxygen Annealed $Sr_3Co_2O_{6.06}$ (Å)

Atom–Atom	Distance (Å)
Sr1–O1	2.618(1) × 8
Sr1–O3	2.710(1) × 4
Sr2–O1	2.674(6) × 4
Sr2–O2	2.404(17) × 1
Sr2–O2	2.731(17) × 4
Co–O1	1.929(2) × 4
Co–O2	1.982(18) × 1
Co–O3	2.006(12) × 1[a]

[a] Partially occupied site.

ing high. The O7 and O8 occupancies refined to constant values where they were fixed after several cycles of refining the temperature factor and occupancy separately. Final stages of the refinement included tying the temperature factors of like atoms on similar sites.

The refinement of peak parameters for the oxygen-annealed sample, $Sr_3Co_2O_{5.94}$, was quite complex. Fitting of the reflections at short *d*-spacing was initially difficult due to the extensive number of closely spaced reflections. Therefore, the peak shape was initially fitted by refining the high *d*-spacing data, where there are more unique reflections and then, in the latter stages of refinement, including the low *d*-spacing data. The O7 and O8 sites occupancies refined to partial occupancy at 39% and 77% occupancy, respectively. The refinement parameters are tabulated in Table 5. Calculated bond distances are tabulated in Tables 6a and 6b for strontium and cobalt, respectively. Important bond angles around the cobalt center are given in Table 6c.

Refinement of the air-quenched sample was more difficult due to broadening of the 001 reflections. This is likely to be a result of stacking faults in the long axis direction (13) which can be observed in many materials with one crystallographic axis much longer than the others. For example, the repeat in $A_3B_2O_7$ is K_2NiF_4 : perovskite : K_2NiF_4 : perovskite. A stacking fault may involve K_2NiF_4 : perovskite : perovskite : K_2NiF_4, i.e., a portion of $A_4B_3O_{10}$ structure. For this reason, the oxygen-annealed sample was initially refined and used as a basis for the refinement of the air-quenched sample. The occupancy of the O7 and O8 sites refined to give 42 and 52% occupancy, respectively. Final refined atomic parameters are summarized in Table 7 and the calculated bond

TABLE 5
Refined Atomic Parameters for $Sr_3Co_2O_{5.94}$

	Site	*x*	*y*	*z*	B_{eq}	Occupancy
Sr1	2*a*	0	0	0	1.14(5)	1.00
Sr2	4*g*	0	0.3365(8)	0	1.14(5)	1.00
Sr3	4*i*	0	0	0.1819(5)	1.14(5)	1.00
Sr4	8*l*	0	0.3299(5)	0.1806(2)	1.14(5)	1.00
Co1	4*i*	0	0	0.5929(9)	0.39(7)	1.00
Co2	8*l*	0	0.3249(5)	0.6007(5)	0.39(7)	1.00
O1	8*l*	0	0.1672(6)	0.4081(3)	0.32(2)	1.00
O2	8*l*	0	0.1644(7)	0.0912(4)	0.32(2)	1.00
O3	4*j*	½	0	*z*	—	—
O4	4*j*	½	0	0.4081(3)	0.32(2)	1.00
O5	4*i*	0	0	0.6910(5)	0.32(2)	1.00
O6	8*l*	0	0.3267(6)	0.6940(2)	0.32(2)	1.00
O7	2*c*	0	0	½	0.32(2)	0.39(4)
O8	4*h*	0	0.3389(10)	½	0.32(2)	0.77(2)

Note. a = 3.8379(1) Å, b = 11.4898(5) Å, c = 20.0812(9) Å, R_{wp} = 8.71, R_{exp} = 4.97, χ^2 = 3.06; refined oxygen content = 5.97(8).

TABLE 6a
Calculated Strontium–Oxygen Bond Distance (Å)

	$Sr_3Co_2O_{5.94}$	$Sr_3Co_2O_{5.78}$
Sr1–O2	2.631(8) × 4	2.708(5) × 4
Sr1–O8	2.666(4) × 4[a]	2.730(8) × 4[a]
Sr2–O1	2.663(4) × 4	2.615(1) × 4
Sr2–O2	2.695(14) × 2	2.701(13) × 2
Sr2–O4	2.633(8) × 2	2.592(8) × 2
Sr2–O7	2.685(6) × 2[a]	2.717(6) × 2[a]
Sr2–O8	2.783(11) × 2[a]	2.761(10) × 2[a]
Sr3–O2	2.624(6) × 2	2.601(6) × 2
Sr3–O5	2.552(14) × 1	2.497(7) × 1
Sr3–O6	2.768(5) × 4	2.727(4) × 4
Sr4–O1	2.618(5) × 2	2.726(3) × 2
Sr4–O2	2.615(9) × 1	2.603(7) × 1
Sr4–O4	2.664(7) × 1	2.713(8) × 1
Sr4–O5	2.747(4) × 2	2.723(5) × 2
Sr4–O6	2.652(6) × 2	2.729(6) × 2
Sr4–O6	2.501(6) × 1	2.518(6) × 1

[a] Partially occupied site.

TABLE 6b
Calculated Cobalt–Oxygen Bond Distances (Å)

	$Sr_3Co_2O_{5.94}$	$Sr_3Co_2O_{5.78}$
Co1–O1	1.911(7) × 2	1.917(6) × 2
Co1–O4	1.919(1) × 2	1.947(2) × 2
Co1–O5	1.970(21) × 1	1.958(19) × 1
Co1–O7	1.866(18) × 1[a]	1.995(18) × 1[a]
Co2–O1	1.831(9) × 1	1.954(15) × 1
Co2–O2	1.932(1) × 2	1.934(1) × 2
Co2–O6	1.874(11) × 1	1.924(11) × 1
Co2–O8	2.029(10) × 1[a]	2.024(10) × 1[a]

[a] Partially occupied site.

TABLE 6c
Calculated Bond Angles Around Cobalt (°)

Atom–Atom–Atom	$Sr_3Co_2O_{5.94}$	$Sr_3Co_2O_{5.78}$
O1–Co1–O1	178.8	165.2
O1–Co1–O4	90.0	89.0
O1–Co1–O5	90.6	97.4
O1–Co1–O7	89.4	82.6
O4–Co1–O5	91.6	98.1
O4–Co1–O7	88.4	81.9
O5–Co1–O7	180.0	180.0
O1–Co2–O2	93.0	88.9
O1–Co2–O6	96.4	96.4
O1–Co2–O8	89.0	84.2
O2–Co2–O6	95.7	92.6
O2–Co2–O8	84.0	87.4
O6–Co2–O8	174.6	179.5

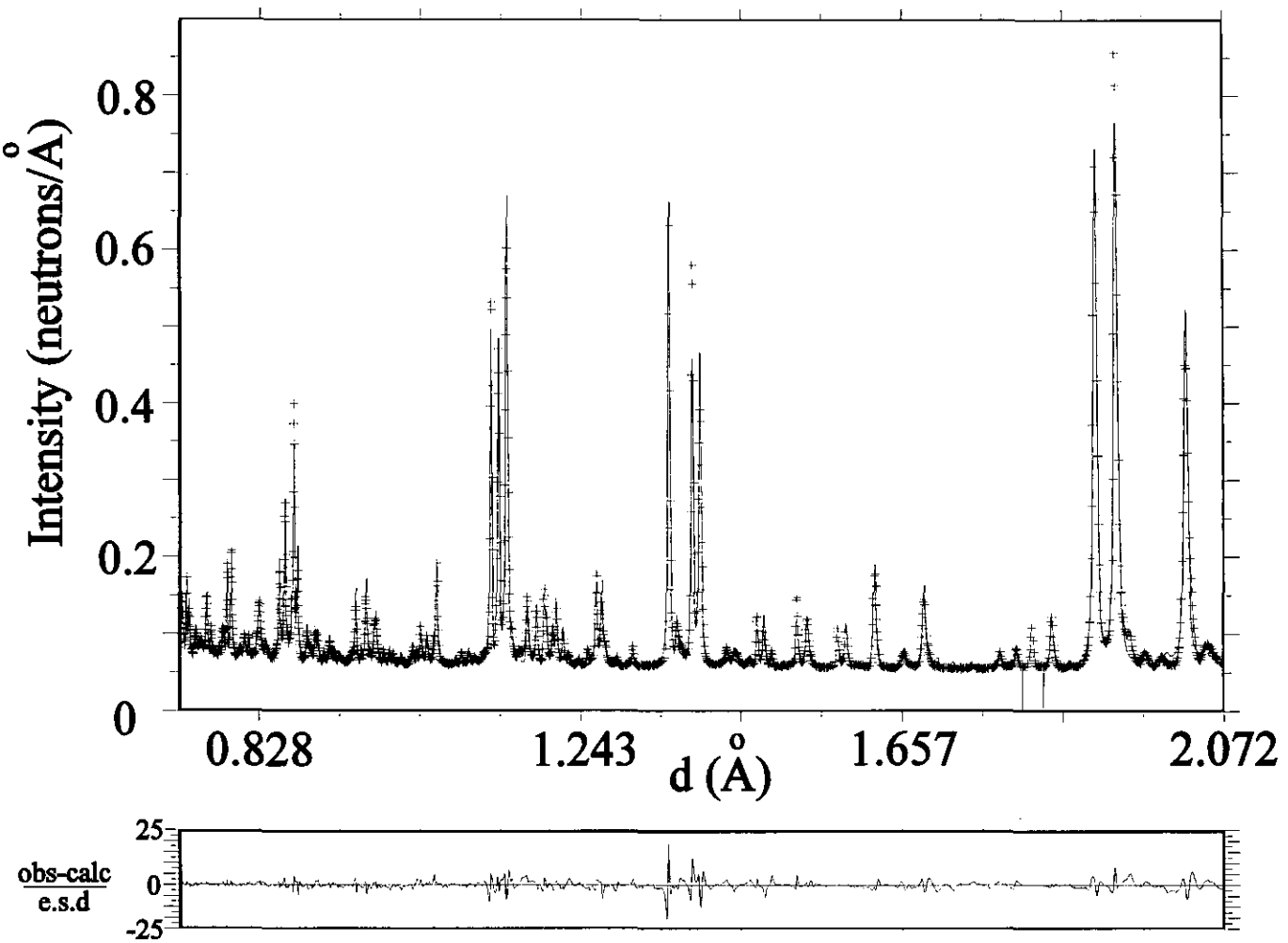

FIG. 4. The fit to the neutron powder diffraction profile of $Sr_3Co_2O_{5.78}$. The upper broken line represents the experimental data and the upper continuous line represents the calculated pattern. The lower continuous line represents the fit on a different scale.

distances for strontium and cobalt in Tables 6a and 6b. Derived bond angles around the cobalt are given in Table 6c. The profile fit is shown in Fig. 4 and a diagram of the structure is depicted in Fig. 5.

Attempts to refine the samples in a smaller crystallographic cell, without tripling the unit cell in the *b*-direction, and in other space groups were unsuccessful with much poorer fit parameters and many of the high *d*-spacing reflections unaccounted for in the profile refinement.

DISCUSSION

Refinement of the tetragonal $Sr_3Co_2O_{6.06}$ sample was successfully achieved in the space group *I*4/*mmm* using powder X-ray data. Comparison of this sample with the trivalent iron analogue, $Sr_3Fe_2O_6$, shows some notable differences. The iron system has a completely vacant O3 site and the apical Fe–O2 distance is very short (1.886 Å) with four Fe–O1 equatorial bonds of 1.980 Å. In the cobalt sample there are four short equatorial bonds at 1.929 Å with two long apical distances of Co–O2 (1.980 Å) and Co–O3 (2.006 Å). The comparatively long distances in the *c*-axis direction are a good indication that there is indeed oxygen on the O3 site: in the iron system there is a large expansion in the *c*-axis direction when the O3 site becomes occupied and the Fe–O1, Fe–O2 distances become more similar. For example in $Sr_3Fe_2O_{6.58}$ the Fe–O2 distance becomes 1.933 Å with four Fe–O1 bonds at 1.942 Å. On this basis, if the O3 site was totally vacant the Co–O2 distance would be expected to be considerably shorter. Bond valence calculations on the cobalt and strontium sites using the parameters for the *divalent* ions give 2.12 for Sr1, 2.11 for Sr2, and 2.62 for Co. This suggests the valence of the cobalt site is greater than two since the divalent ion would be extremely overbonded on this site. This implies that the cobalt ions are in the triva-

lent state; calculated bond valence parameters for ions in an $n + 1$ oxidation state using the A^{n+} bond valence parameter generally give values of $n + 0.6/7$. Both calculated valences for the strontium sites are in good agreement with the theoretical oxidation state of strontium of two. Refinement of the oxygen occupancy suggested a small amount of oxygen (occupancy = 0.13) on the O3 site which gave excellent agreement with the analytically determined oxygen stoichiometry of 6.06(5). However, it should be noted that the esd on this occupancy is large, giving a value which lies within three esd's of zero and may indicate a very low occupancy.

Refinement of the tripled structures using the refinement of *X*-ray data was not ideal due to the complexity of the structure and the paucity of the data. However, characterization of the heavy atom sites was possible, but, in general, gave poor agreement with that of the neutron diffraction results. The X-ray refinement is unfavorably affected both by the form factor and by X-ray fluorescence resulting from the use of copper radiation. Refinement of $Sr_3Co_2O_{7-z}$ samples using powder neutron diffraction from HRPD, however, gave much better results due to the high quality and quantity of data. The structure was successfully refined in the space group *Immm* and shows evidence of a complex oxygen-ordering mechanism. A comparison of the typical Ruddlesden–Popper cell and the tripled cell coordinates derived from this unit cell is shown in Table 8. Cation positions in the tripled unit cell are displaced only very slightly from the positions created by stacking three tetragonal unit cells together. This suggests that the tripled structure is a result of oxygen ordering. This is in contrast with the tripled structure of *Ln*636 cuprates, where both cation and oxygen ordering are clearly evident. As previously noted in the *Ln*212 systems (11), the tripled structure occurs only when there is a large amount of strontium present. Strontium is unusual in that it can sustain a variety of coordination numbers, i.e., 6-, 7-, 8-, 9-, 10, and 12-fold are all known. In $Nd_{1.4}Sr_{1.6}Cu_2O_{5.79}$, the A1 and A3 low coordination sites are filled by the neodymium with Sr on the 12-fold A2 site and a mixture of the two ions on the A4 site. The lowest coordination number in the tripled *Ln*212 structure is 7; strontium can exist in this coordination environment and, indeed, any other coordination environment present in 636. Bond valence (14) calculations on the strontium and cobalt sites are summarized in Table 9.

It can be seen that Sr is underbonded on the A1 and A3 sites which are the low coordinate eight- and sevenfold

TABLE 7
Refinement Parameters for $Sr_3Co_2O_{5.78}$

	Site	x	y	z	B_{eq}	Occupancy
Sr1	2*a*	0	0	0	1.52(3)	1.00
Sr2	4*g*	0	0.3330(8)	0	1.52(3)	1.00
Sr3	4*i*	0	0	0.1818(3)	1.52(3)	1.00
Sr4	8*l*	0	0.3339(6)	0.1819(2)	1.52(3)	1.00
Co1	4*i*	0	0	0.5984(9)	1.12(6)	1.00
Co2	8*l*	0	0.3356(12)	0.5998(5)	1.12(6)	1.00
O1	8*l*	0	0.1663(5)	0.4130(1)	1.01(2)	1.00
O2	8*l*	0	0.1669(5)	0.0947(2)	1.01(2)	1.00
O3	4*j*	½	0	*z*	—	0
O4	4*j*	½	0	0.4136(3)	1.01(2)	1.00
O5	4*i*	0	0	0.6950(2)	1.01(2)	1.00
O6	8*l*	0	0.3330(5)	0.6947(2)	1.02(2)	1.00
O7	2*c*	0	0	½	1.02(2)	0.42(2)
O8	4*h*	0	0.3314(10)	½	1.02(2)	0.52(1)

Note. a = 3.8631(1) Å, b = 11.4319(1) Å, c = 20.2265(1) Å, R_{wp} = 8.87, R_{exp} = 2.74, χ^2 = 10.49; Refined oxygen content = 5.82(2).

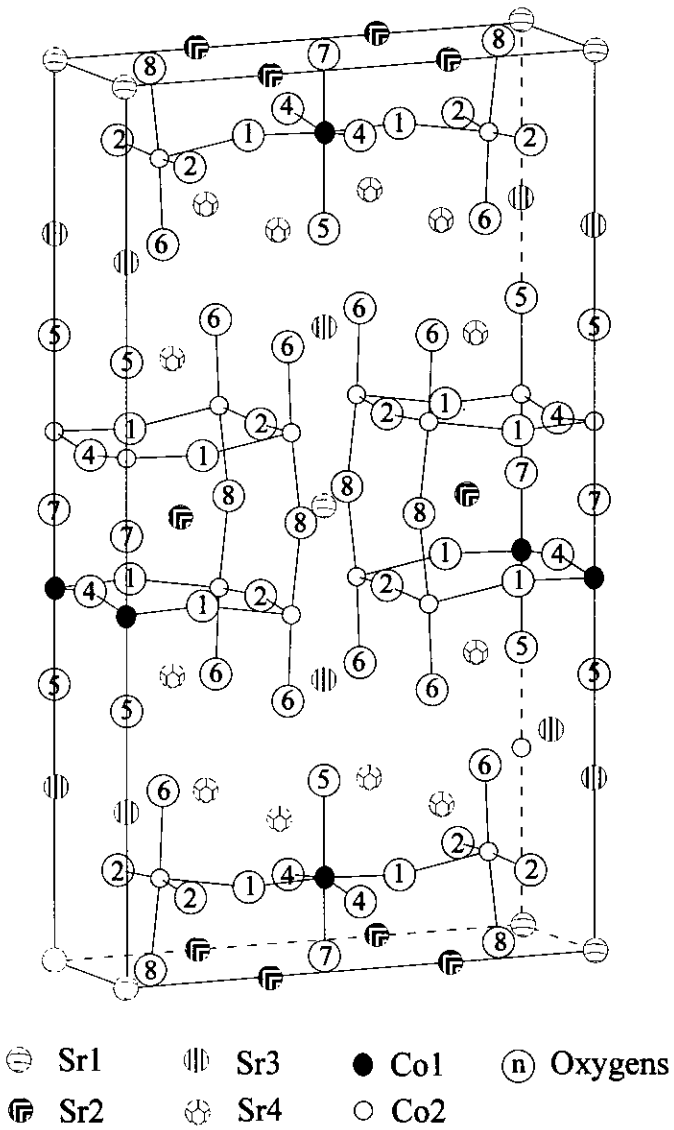

FIG. 5. The tripled structure of $Sr_3Co_2O_{5.78}$ showing the various strontium and cobalt sites.

TABLE 8
Relative Positional Coordinates of Ruddlesden–Popper $A_3B_2O_7$ and the Tripled Phases

Ruddlesden–Popper				Tripled Cell				5.94	5.78
Sr1	0	0	0	Sr1′	0	0	0		
				Sr2′	0	$\frac{1}{3}+*$	0	* = 0.0032	* = −0.0003
Sr2	0	0	z	Sr3′	0	0	z^1		
				Sr4′	0	$\frac{1}{3}+*$	z^2	* = −0.0034	* = 0.0006
B	0	0	z^i	B1′	0	0	z^3		
				B2′	0	$\frac{1}{3}+*$	z^4	* = −0.084	* = 0.0024
O1	0	$\frac{1}{2}$	z^{ii}	O1′	0	$\frac{1}{6}+*$	z^5	* = 0.0006	* = −0.0003
				O2′	0	$\frac{1}{6}+*$	$\frac{1}{2}$-z^6	* = −0.022	* = 0.0003
				O3′	$\frac{1}{2}$	0	z^7		
				O4′	$\frac{1}{2}$	0	z^8		
O2	0	0	z^{iii}	O5′	0	0	z^9		
				O6′	0	$\frac{1}{3}+*$	z^{10}	* = 0.0066	* = 0.0003
O3	0	0	$\frac{1}{2}$	O7′	0	0	$\frac{1}{2}$		
				O8′	0	$\frac{1}{3}+*$	$\frac{1}{2}$	* = 0.0056	* = 0.0019

Note. * indicates different increments.

sites. A better situation is achieved on the A2 and A4 sites. The site valence for Sr1, Sr2, and Sr4 is more acceptable in the oxygen-annealed sample, and this may be a result of oxygen ordering where the air-quenched sample will be affected by disorder. However, bond valence parameters are calculated for each atom in many different structures and as a result will be most appropriate for the most common coordination numbers; i.e., for strontium this is 12. The low values obtained for the seven- and eight-coordination sites must therefore be treated with caution. In both cases the calculated valence of the cobalt sites is significantly elevated above 2, suggesting the sites are very overbonded for a divalent cobalt ion. The high values for the cobalt valence imply these sites are accommodating a large proportion of cobalt(III). In both cases the sixfold site (Co1) has a higher calculated valence than the fivefold (Co2) site. In the oxygen-annealed sample, where oxygen ordering has time to occur, this situation is accentuated.

Another property of the tripled cuprate structures which is emphasized in this system is the behavior toward oxygen. For example in the $Sm_{1.3}Sr_{1.7}Cu_2O_{6\pm y}$ (11) system very marginal oxygen uptake occurs on annealing and the lattice parameters remain the same within the limits of experimental error. The ability to pick up extra oxygen increases with lanthanides greater in size than strontium, but has not yet been possible above six in these cuprates. However, in the normal Ruddlesden–Popper phase, an oxygen level of six is readily obtained. The small degree of oxidation in the $Sm_{1.3}Sr_{1.7}Cu_2O_{6\pm y}$ causes a contraction of both a- and b-axes with the former being more prominent. This process is consistent with oxygen being placed on the O3 or O7 site. Different behavior is noted in the cobalt system: the largest contraction is in c with a small decrease in a and an increase in b.[3] Considering the two samples prepared under different conditions it can be seen that although the occupancy of the O7 site remains constant within the limits of experimental error there is a large change in the occupancy of the O8 site which, in conjunction with O7, has the largest affect on the c-axis. However, during this process the average Co2–O8–Co2 distance changes very little, where a shortening would be indicative of filling the O8 site. The other apical distance, Co2–O6, shrinks by 0.05 Å during the oxidation, which is consistent with an increase in the valence of the Co2 ion. An explanation for this change in the coordination environment of the O2 ion lies in the other atoms coordinated to the O8 atoms. The part of the structure containing the Co2–O8 distance is already under compression: further shortening of the bond is disfa-

TABLE 9
Calculated Site Valences

Atom	$Sr_3Co_2O_{5.78}$	$Sr_3Co_2O_{5.94}$
Sr1	1.40	1.70
Sr2	2.40	2.08
Sr3	1.68	1.51
Sr4	2.35	2.20
Co1	2.65	3.00
Co2	2.38	2.65

vored due to the associated increase in the already overbonded Sr2 bond valence. This process increases the Sr2–O8 distance and gives Sr2 a more acceptable coordination. At the same time the Co1–O7–Co1 distance decreases by 0.26 Å indicating a contraction into the perovskite blocks. The strontium atoms in the NaCl type layers (Sr3, Sr4) experience a drop in the calculated bond valence. In both the oxygen-annealed and air-quenched samples there is overwhelming evidence that the O3 site is vacant.

Low-temperature annealing of $Sr_3Co_2O_{7-y}$ in oxygen causes a phase change to the tetragonal system when the oxygen content rises above 6 as seen in the analogous copper system. However, attempts to introduce further oxygen, through for example high pressure annealing, causes the structure to fall apart completely to give a mixture of the hexagonal phase, $SrCoO_{2.7}$ and SrO. This is probably the result of an attempt to further contract in the $AlCo(1)O_{3-\delta}$ and $A4Co(2)O_{3-\delta}$ blocks. On annealing all the bonding distances around the Sr3 atom in the NaCl layer increase, leading to a drop in the bond valence of the Sr3 site. Assuming this situation would continue to worsen on increasing the oxygen level than eventually the structure would no longer be stable and would fall apart. All these phases have shown sensitivity to atmospheric conditions. This is similar to the iron system, where the phases $Sr_3Fe_2O_{6.58}$ and $Sr_3Fe_2O_{6.75}$ are both extremely sensitive to atmospheric moisture. This phenomenon is clearly not due just to the instability of the tetravalent ion, since the pure iron(IV) sample has a much extended lifetime under the same conditions. Considering all the samples, the common characteristic of all the samples of both cobalt and iron showing poor resistance to atmospheric conditions is a long c-axis. The long c-axis is a feature of compounds with partial oxygen vacancy on the sites controlling the interplanar B–B distance. This suggests a tendency to react with the atmosphere in order to fill the deficient coordination sphere; this is most facile when the interplanar distance is large.

CONCLUSIONS

A new phase with the Ruddlesden–Popper, $Sr_3Ti_2O_7$, structure has been shown to exist for cobalt. The $Sr_3Co_2O_{7-y}$ system hosts a wide range of oxygen stoichiometry with $0.94 \leq y \leq 1.22$. At high values of y, the system crystallizes orthorhombic in the space group $Immm$ with a threefold tripling of the Ruddlesden–Popper phase along b. This property is also exhibited by the semiconducting cuprate phases, $Ln_{2+x}Sr_{1+x}Cu_2O_{6-y}$ (Ln = Gd, Sm and Eu), where the tripling is a direct result of cationic ordering and the ordering of oxygen vacancies. In contrast, the cobalt system is tripled due to oxygen vacancy ordering only. The O3 site is completely vacant with partial occupancy on the O7 and O8 sites. This generates both octahedral and square-pyramidal cobalt sites. Increasing the oxygen content, lowering y, can be achieved by oxygen annealing at temperatures in excess of 1000°C and causes a phase change to tetragonal. The normal Ruddlesden–Popper phase is now restored and the cobalt sites are mostly square-pyramidal (87%) with the remainder (13%) have octahedral coordination. Increasing the oxygen content further by oxygen annealing at temperatures below 500°C causes the crystallinity of the samples to deteriorate and the appearance of impurity phases.

Refinements to determine the crystal structure of these materials were achieved using the Rietveld method. This gives an averaged picture of the whole structure; therefore to fully characterize the local structure, a technique such as EXAFS, which studies the local coordination of ions, would be required.

ACKNOWLEDGMENTS

We thank the SERC for the studentship for S.E.D., and Dr. D. B. Currie for his assistance in the high pressure work.

REFERENCES

1. I. S. Shaplygin and V. B. Lazerev, *Russ. J. Inorg. Chem. Engl. Transl.* **30,** 3214 (1985).
2. J. B. MacChesney, R. C. Sherwood, and J. F. Potter, *J. Chem. Phys.* **43,** 1908 (1965).
3. A. N. Petrov, V. A. Chereparov, O. F. Konochuk, and L. Ya. Govnlova, *J. Solid State Chem.* **87,** 69 (1990).
4. H. Takei, H. Oda, and H. Watanabe, *J. Materials. Sci.* **13,** 519 (1978).
5. S. E. Dann, D. B. Currie, and M. T. Weller, *J. Solid State Chem.* **92,** 237 (1991).
6. S. E. Dann, D. B. Currie, and M. T. Weller, *J. Solid State Chem.* **97,** 179 (1992).
7. D. Baltz and K. Pleith, *Z. Electrochem.* **59,** 545 (1951).
8. S. N. Ruddlesden and P. Popper, *Acta Crystallogr.* **4,** 503 (1951).
9. N. Nguyen, L. Er-Rakho, C. Michel, J. Choisnet, and B. Raveau, *Mater. Res. Bull.* **15,** 891 (1980).
10. N. Nguyen, C. Michel, J. Choisnet, and B. Raveau, *Mater. Res. Bull.* **17,** 567 (1982).
11. J. R. Grasmeder and M. T. Weller, *J. Solid State Chem.* **85,** 88 (1990).
12. H. M. Rietveld, *Acta Crystallogr.* **22,** 151 (1967).
13. J. Drennan, C. P. Tavares, and B. C. H. Steele, *Mater. Res. Bull.* **17,** 62 (1982).
14. I. D. Brown and D. Aldermatt, *Acta. Crystallogr. B.* **41,** 244 (1985).